

# Automatic Maize Leaf Disease Recognition Using Deep Learning

Muhammet ÇAKMAK<sup>1</sup> 

<sup>1</sup>Sinop University, Department of Computer Engineering, Sinop, Türkiye

Corresponding author:

Muhammet Çakmak, Sinop University,  
Department of Computer Engineering  
mcakmak@sinop.edu.tr



Article History:

Received: 12.01.2024

Accepted: 18.03.2024

Published Online: 18.03.2024

## ABSTRACT

Maize leaf diseases exhibit visible symptoms and are currently diagnosed by expert pathologists through personal observation, but the slow manual detection methods and pathologist's skill influence make it challenging to identify diseases in maize leaves. Therefore, computer-aided diagnostic systems offer a promising solution for disease detection issues. While traditional machine learning methods require perfect manual feature extraction for image classification, deep learning networks extract image features autonomously and function without pre-processing. This study proposes using the EfficientNet deep learning model for the classification of maize leaf diseases and compares it with another established deep learning model. The maize leaf disease dataset was used to train all models, with 4188 images for the original dataset and 6176 images for the augmented dataset. The proposed models were compared with ResNet50, VGG19, DenseNet121 and Inception V3 models according to their accuracy, sensitivity, F1-Score and precision values. The EfficientNet B6 model achieved 98.10% accuracy on the original dataset, while the EfficientNet B3 model achieved the highest accuracy of 99.66% on the augmented dataset.

**Keywords:** Deep learning, Transfer learning, Plant disease classification

## 1. Introduction

Precisely detecting diseases in maize leaves is critical to sustain food policies and ensure proper agricultural practices. In addition, early detection of diseases in the leaves of maize plants is of great importance in preventing time and financial losses. Some maize leaf diseases are difficult to diagnose because they have no outward signs of disease. However, most maize leaf diseases show visible symptoms. Typically, an expert pathologist diagnoses diseases on maize leaves through visual observation [1]. When diagnosing maize leaf diseases, a plant pathologist must observe the characteristic symptoms of the disease. Experienced pathologists may still struggle to diagnose certain diseases, as climate change and the rapid spread of maize leaf diseases to previously unaffected regions can alter disease courses and make accurate diagnosis challenging [2].

Applications of the machine and deep learning models in many fields, such as insect detection [3], fungus detection [4], healthcare [5], [6], [7], [8], and education [9], are rapidly increasing. Developing intelligent systems capable of automatically and precisely diagnosing maize leaf diseases benefits engineers seeking to boost production. Moreover, creating a mobile application that can assist farmers struggling with diseases and lacking technical support infrastructure is a significant advancement [10]. Recent advances in deep learning models have enabled the creation of systems that can accurately and quickly classify plant species and diagnose plant diseases. Currently, artificial intelligence techniques in plant disease classification and diagnosis are widespread [11]. Over the last ten years, numerous artificial intelligence models have been suggested for identifying and detecting plant diseases [12], [13], [14]. In their study, the authors employed the Support Vector Machine (SVM) algorithm to identify and classify diseases in sugar beet crops. [11]. Al-Hiary et al. deduced the texture and color characteristics of the diseased areas in 5 different plant leaves using K-means. They then classified the diseases from the obtained features using an Artificial Neural Network [15]. The authors of a different study proposed a Particle Swarm Optimization approach for classifying cotton leaf diseases. This method selects features based on texture, edge, and color using particle swarm optimization, and a cross-information neural network is used to classify the six types of cotton leaf diseases [16]. Mokhtar et al. identified the disease-causing virus species in tomato leaves using the Support Virtual Machine [17]. The authors used SVM to identify the disease in three grapevine leaves [18]. Johannes et al. proposed a mobile-based software that uses a Naive Bayes classifier to detect images of wheat diseases [19]. Chen et al proposed an automated disease recognition logistic algorithm using the group method to detect plant diseases [20]. The feature extraction process is a critical

issue in machine learning, as it can significantly impact classification accuracy. Advances in technology have resulted in significant increases in the speed and capacity of graphics processing units and central processing units, which have facilitated the development of deep learning methods that can achieve high performance without the need for manual feature extraction [21], [22].

Many processing layers and neurons in deep neural networks allow them to efficiently process large and complex data, such as image and voice recognition tasks [23]. As a result, deep learning methods are frequently used to detect medical diseases [24], [25], [26]. Bozkurt F. used a handcrafted features-based framework to diagnose COVID-19 [27]. On the other hand, there is a growing trend in utilizing deep learning techniques for detecting and classifying plant diseases [28]. Chen et al. proposed an ensemble network named Es-MbNet, which was developed by combining three lightweight CNNs, utilizing transfer learning and a two-stage training approach to enhance the identification of subtle plant lesion features, achieving an impressive average accuracy of 99.37% on a local dataset and 99.61% on the PlantVillage dataset [29]. Another study conducted by Chen et al. utilized VGG deep learning architecture to detect diseases in maize and rice leaves, achieving accuracy rates of 91.83% and 92%, respectively [30]. The study introduces CoffeeNet, a novel deep-learning model tailored for the early detection and categorization of various coffee plant leaf infections, addressing challenges posed by image distortions such as color variations, lighting changes, and size alterations. Leveraging a spatial channel attention strategy based on the ResNet-50 model within the CenterNet framework, CoffeeNet achieves an impressive classification accuracy of 98.54% and a mean Average Precision (mAP) of 0.97, demonstrating its efficacy in localizing and categorizing complex coffee leaf anomalies [31]. Too et al. employed VGG16, ResNet152, ResNet101, ResNet50, and DenseNets121 deep learning methods to detect leaf diseases. Among these methods, DenseNets121 achieved the highest accuracy of 99.75%, owing to its efficient computation time and reduced number of parameters [32]. In a separate study, the authors proposed a 9-layer CNN architecture for classifying plant diseases. They compared this method with logistic regression, SVM, K-NN, and decision trees. The authors used a dataset of 55,636 images and 39 classes for testing and training. The proposed CNN network achieved a classification accuracy of 96.46% in identifying plant diseases [33]. In another research, vision transformer (ViT)-like techniques are employed for plant disease identification, introducing an innovative edge-feature guidance (EFG) module that enhances the extraction of localized features. Through integration with leading methods like ViT, PVT, and Swin, the proposed ViT-based EFG module demonstrates superior feature extraction performance and outperforms existing models across Paddy, Wheat, Cabbage, and Coffee datasets [34]. Kusumo et al. (year) employed speeded-up robust features (SURF), Oriented FAST, scale-invariant feature transform (SIFT), and object detector methods such as histogram of oriented gradients. They rotated BRIEF (ORB) to detect RGB colors in maize leaves. The authors compared these features with Naive Bayes (NB), SVM, Random Forest (RF), and Decision Tree (DT) methods [35]. Hassan et al. proposed two classification methods for diseases of maize, potato, and tomato plants: shallow VGG with Xgboost and shallow VGG with RF and deep learning networks. The authors found that Xgboost yielded the highest accuracy rate in classifying maize, potato, and tomato leaf defects with rates of 94.47%, 98.74%, and 93.91%, respectively [36]. Atilla et al. utilized various CNN models, including AlexNet, ResNet50, VGG16, Inception, and EfficientNet, to classify 54,305 images of plant diseases with an accuracy of 98.42% [37]. Fayyaz et al. proposed a CNN architecture that combines SqueezeNet and ShuffleNet for early detection of leaf blight in plants. The authors also employed SVM for classification and the CIELAB color space to enhance accuracy. They achieved a 98% accuracy rate in classifying leaf blights [23]. Elaraby and colleagues classified 25 plant leaf diseases using AlexNet and Particle Swarm optimization. The proposed deep learning architecture achieved an accuracy rate of 98.93% in classifying plant diseases [39]. As noted in the literature, the utilization of machine learning and deep learning techniques for diagnosing plant diseases is rapidly expanding. However, there are still gaps in applying new deep-learning architectures to detect diseases in maize leaves. Specifically, there is a need for models that can be trained quickly, have fewer parameters, and exhibit high performance.

The current study presents a deep learning architecture for classifying maize leaf diseases, utilizing a CNN EfficientNet. The proposed CNN architecture is then compared to ResNet50, VGG19, DenseNet121, and Inception V3 CNN architectures. The remaining sections of this study are structured as follows: Section 2 describes the dataset used and the deep neural network architectures employed. In contrast, Section 3 outlines the experimental methodology. Section 4 presents the study's results and provides a detailed discussion of the findings, and the study is ultimately concluded in Section 5.

## 2. Materials and Methods

### 2.1 Dataset

This research used a dataset of maize leaf diseases, which comprised 4,188 images of colored leaves with varying sizes. The dataset included four categories of maize leaves, of which 1306 images represented Common Rust, 574 images represented Gray Leaf Spot, and 1146 images represented Blight maize leaf disease. Additionally, 1162 images represented healthy maize leaves. The dataset was composed of three diseased maize leaves and one healthy maize leaf. Figure 1 displays original dataset images of four types of maize leaf diseases as well as healthy and diseased leaves.



Figure 1 Original dataset: a) Common rust disease, b) Blight disease, c) Gray spot disease, d) Healthy leaves

The dataset used in this study was augmented using various techniques, resulting in 5932 images. Horizontal flip, 20% rotation, 20% width shift, 20% height shift, and zoom were applied to create the augmented dataset. Figure 2 shows visual representations of the maize leaf images in the augmented dataset.

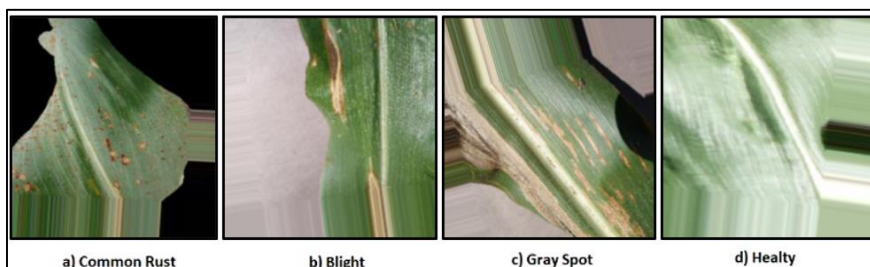


Figure 2 Augmented dataset: a) Common rust disease, b) Blight disease, c) Gray spot disease, d) Healthy leaves

### 2.2 Transfer Learning

Transfer learning is a machine learning technique that involves leveraging the knowledge acquired from solving a previous problem to tackle a new and similar problem. In traditional machine learning, the learning process occurs while performing different tasks [40]. However, transfer learning involves utilizing source tasks obtained from machine learning methods for new tasks [41]. Figure 3 illustrates the schematic representation of traditional and transfer learning. Transfer learning utilizes the knowledge gained from a pre-trained network, leading to higher accuracy and time savings than training the model from scratch.

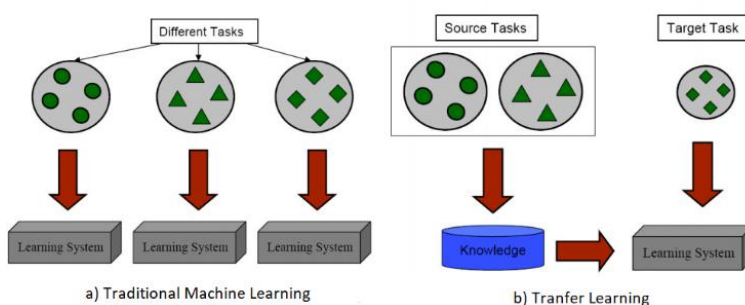


Figure 3 Schematic representation of traditional and transfer learning [41]

### 2.3 Deep Learning Models

In this study, the comparative performance of the proposed EfficientNet deep learning architecture has been evaluated against several state-of-the-art CNN architectures, including ResNet50, VGG19, DenseNet121, and Inception V3.

#### 2.3.1 ResNet50

The Residual Networks (ResNets) were developed to overcome the challenges posed by numerous non-linear layers, such as not being able to learn identity maps and the problem of degradation. The ResNets architecture aims to ease the network's

training process. ResNet50 is a model with many stacked units consisting of pooling and convolution layers. This model has a depth of 50 layers and 26M parameters and employs 3×3 filters for input images of 224×224 pixels [42]. It uses skip connections to allow the propagation of information across layers. Additionally, the ResNet50 architecture has one MaxPooling layer, one Average Pooling layer, and 48 Convolution layers. Figure 4 illustrates the schematic ResNet50 architecture.

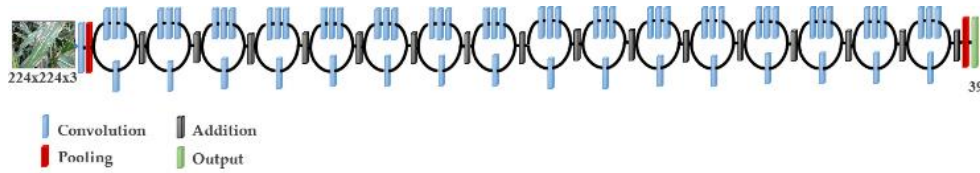


Figure 4 ResNet50 schematic architecture [42]

### 2.3.2 VGG19

The VGG architecture was developed to enable deep convolutional networks to recognize large-scale images. The VGG19 model, a variant of the VGG architecture, comprises 5 MaxPooling layers, 16 convolution layers, 3 Fully Connected layers, and 1 SoftMax layer. VGG19 achieved the top rank in the Large-Scale Visual Recognition Competition (ILSVRC) in 2014 [43]. It has 138 million parameters and was trained on more than one million images. To reduce the number of parameters, VGG19 uses 3x3 kernels. The architecture of VGG19 consists of 19 layers, and its input layer image size is 224x224 pixels. A schematic of the VGG19 architecture is shown in Figure 5.

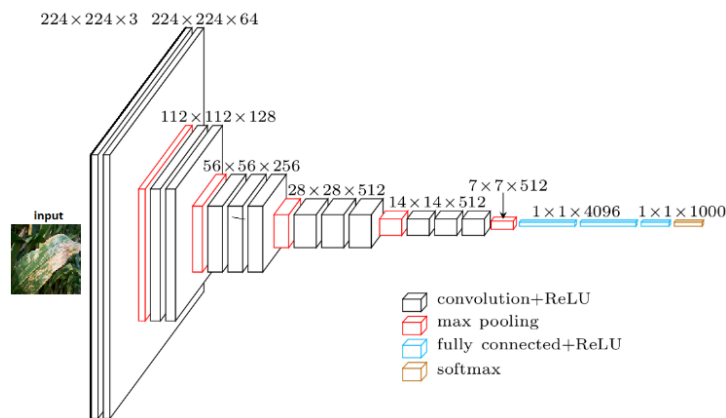


Figure 5 Schematic representation of VGG19 [44]

### 2.3.3 DenseNets121

DenseNets [45] is an architecture that aims to increase the depth of deep convolutional networks and train the network better by establishing short connections between layers. DenseNets uses fewer parameters than other CNN architectures, as there is no need to learn extra feature maps. Also, its layers are very narrow, and only those layers add a small feature map. DenseNets connects directly between layers to improve the flow of information between layers. Figure 6 shows the 5-layer DenseNet block diagram.

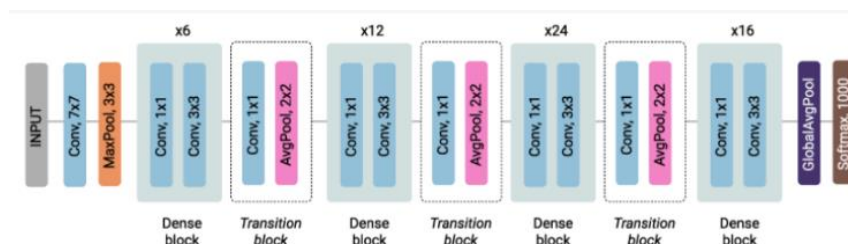


Figure 6 A 5-layer dense block with an expansion rate of k= 4 [45]

The implementation of DenseNet architecture consists of three types of blocks, namely the convolution block, dense block, and transition block. The convolution block, or the main block, connects the dense blocks [46]. The thick block is the main component of DenseNet. Transition blocks are situated between the dense blocks and serve to decrease the dimensionality of the feature map. A schematic illustration of the block structure of the DenseNet architecture is provided in Figure 7. The input layer image size for DenseNet121 is 224x224.

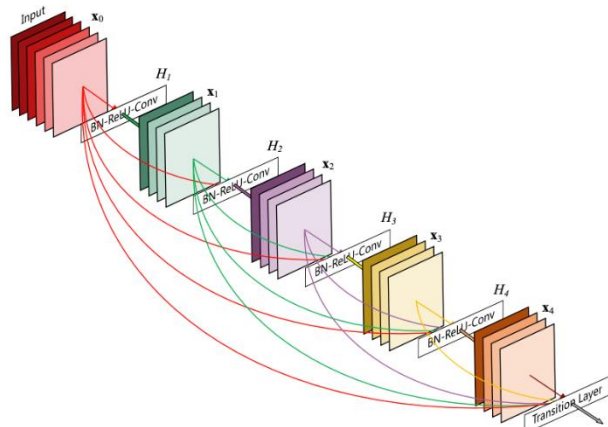


Figure 7 DenseNets block architecture [47]

### 2.3.4 InceptionV3

The Inception architecture initially called GoogleNet in 2014, is a pre-trained network model [25]. Google developed the 3rd Generation of this deep learning architecture, known as Inception V3. Inception V3 uses a factorization approach to improve the deep learning network's performance by reducing the number of parameters and connections [48]. The network structure of Inception V3 comprises various components, such as convolutions, average and maximum pooling, dropouts, concerts, and fully connected layers. This model has a depth of 48 layers and can process images of size 299x299 pixels. The model's architecture is illustrated in Figure 8.

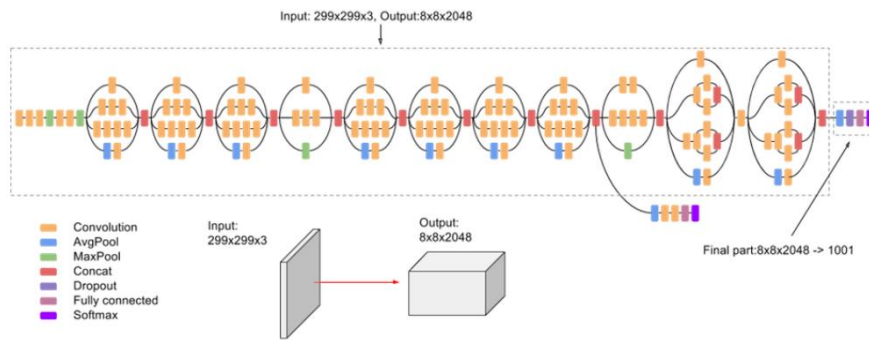


Figure 8 Schematic Inception V3 architecture [49]

### 2.3.5 EfficientNet

The Inception architecture, also known as GoogleNet, is a pre-trained network model that was introduced by Google in 2014 [49]. Inception V3, the third Generation of this architecture, utilizes the factorization method to enhance the deep learning network's performance by minimizing the number of parameters and connections. The network comprises convolutions, average and maximum pooling layers, dropout layers, concatenation layers, and fully connected layers. The Inception V3 model has 48 layers and requires input images of size 299x299 pixels [50]. The model's architectural representation can be seen in Figure 9.

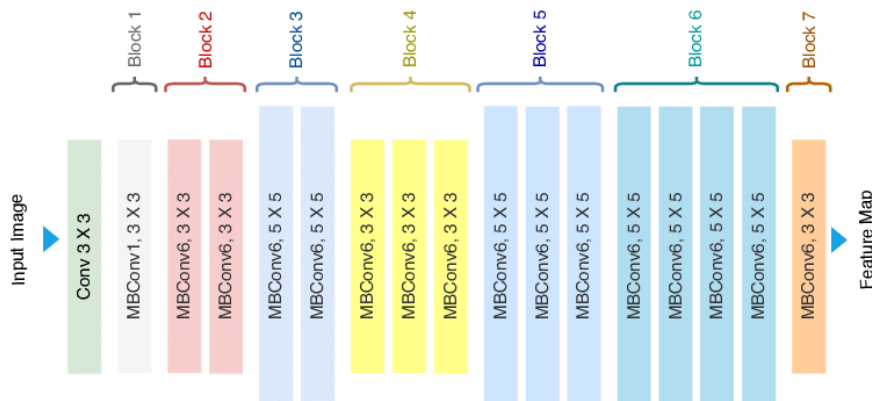


Figure 9 Schematic EfficientNet B0 architecture [41], [51]

### 3. Experimental Study

#### 3.1. Experimental Setup

The deep learning models were trained in the Google cloud environment using a GPU-accelerated system. The training was performed on a Tesla T4 GPU and an Intel Xeon 2.20 GHz CPU with 16 GB RAM. For the transfer learning design, all programs were written in Python 3 programming language, and the Keras 2.3.1 training framework was utilized.

#### 3.2. Training

In this research, we evaluated deep learning models' efficacy in categorizing maize leaf diseases such as Blight, Common Rust, Gray leaf spot, and Healthy, using both original and augmented datasets. Table 1 shows the distribution of training, validation, and test data between these two datasets. The original dataset encompassed 4,188 images, segmented into training, validation, and test groups. Specifically, the training group comprised 3,769 images, accounting for 90% of the dataset, while the validation and test groups had 209 and 210 images, respectively. To enhance model accuracy, we expanded our dataset through diverse image augmentation methods like rotation, scaling, and mirroring. Consequently, the augmented dataset contained 5,932 images partitioned into the same three categories. Notably, the augmented training set consisted of 5,338 images (90% of the total), while both validation and test subsets included 297 images each.

Table 1 Original and augmented data in the dataset

	Total data	Training (90%)	Validation (5%)	Test (5%)
<b>Original dataset</b>	4.188	3.769	209	210
<b>Augmented dataset</b>	5.932	5.338	297	297

In this study, we adopted transfer learning techniques by repurposing established CNN architectures and fine-tuning them to expedite the learning process. To facilitate this, we incorporated the ImageNet dataset, which boasts approximately 1.2 million images spanning 1000 distinct categories, as a foundational basis for transfer learning. Utilizing pre-existing weight values significantly streamlined our deep learning models' training phase. The final Fully Connected (FC) layers across all models were reconfigured to yield four specific outputs tailored to address the objectives of our study. We designated the CNN layers for training while employing Softmax as the chosen activation function and categorical cross-entropy to quantify the loss. Furthermore, to optimize the training regimen, we implemented an early stopping mechanism, maintaining a consistent threshold of 3 and a loss threshold set at 1e-3.

The pre-trained models in this study were optimized using the same optimization method as the ImageNet dataset. Adam's learning rate was 0.001, while SDG was set to 0.01. A validation value limit of 1 was used for all models. Normalization was applied to all image data used in the dataset. The image data was resized to different sizes for each transfer learning model. ResNet50, VGG19, DenseNet121, and EfficientNet B0 were resized to 224x224 pixels, while InceptionV3 was resized to 299x299 pixels. The EfficientNet network models had different input image sizes. To ensure a fair evaluation of all EfficientNet models, a pixel value of 224x224 was selected for our experimental study. The resolution values of the selected models can be found in Table 2. In this research, the batch mechanism was utilized to update the bias and weights in training the models. To comply with the hardware resources, the maximum value of the batch was established as 32.

Table 2 Transfer learning model input value and parameters

Transfer Learning Models	Image Input Values	Model Parameters
ResNet50	224x224	25,636,712
VGG19	224x224	138,357,544
DenseNet121	224x224	7,978,856
InceptionV3	299x299	23,851,784
EfficientNet		
B0	224x224	5,330,571
B1	240x240	7,856,239
B2	260x260	9,177,569
B3	300x300	12,320,535
B4	380x380	19,466,823
B5	456x456	30,562,527
B6	528x528	43,265,143
B7	600x600	66,658,687

We set the bias 11 kernel regularizer value to 0.006 and the bias 12 kernel regularizer value to 0.016 for fine-tuning. ReLu was used as the activation function in the layers, while Softmax was used as the output activation function. We applied a dropout rate of 40%. For batch normalization, we chose a momentum of 0.99 and an epsilon value of 0.001.

### 3.3. Performance Metrics

A multi-class assessment was carried out on the maize leaf dataset, comprising four categories. Model performance was assessed using True Positive (TP), False Positive (FP), True Negative (TN), and False Negative (FN) values derived from the confusion matrix, as depicted in equations (1), (2), (3), and (4). Model comparison was based on F1-Score (F1\_Score), Accuracy (ACC), Sensitivity (Sen), and Precision (Precision) metrics, calculated using equations (1), (2), (3), and (4). For a given class  $x$ ,

$$Sen(x) = \frac{TP(x)}{TP(x) + FN(x)} \quad (1)$$

$$F1\_Score(x) = \frac{2 * Pre(x) * Sen(x)}{Pre(x) + Sen(x)} \quad (2)$$

$$Acc(x) = \frac{TP(x) + TN(x)}{TP(x) + FN(x) + TN(x) + FP(x)} \quad (3)$$

$$Pre(k) = \frac{TP(k)}{TP(k) + FP(k)} \quad (4)$$

## 4. Results and Discussions

Maize is a staple food in many countries, and its cultivation is essential for food security. However, the crop is susceptible to various diseases that can significantly affect its yield. To address this issue, researchers have developed deep-learning models to classify maize leaf diseases from images. In this article, we compare the performance of several deep learning models for maize leaf disease classification, including ResNet50, VGG19, DenseNet121, InceptionV3, EfficientNet B0, B1, B2, B3, B4, B5, B6, and B7.

The research conducted involved utilizing both the original and augmented datasets in all experimental studies. The average results of the original dataset for each model are presented in Table 3, while the outcomes of the augmented dataset are presented in Table 3.

We use the same original dataset to evaluate the models, which contains images of maize leaves affected by Blight, Common Rust, Gray leaf spot, and Healthy. We report the accuracy, sensitivity, F1-score, and precision of each model.

Firstly, ResNet50 achieved an accuracy of 96.67%, making it one of the best-performing models in our comparison. It also achieved a sensitivity of 95.70%, an F1-score of 95.67%, and a precision of 95.66%. These results suggest that ResNet50 is a reliable maize leaf disease classification model.

In contrast, VGG19 had a lower accuracy of 91.43%, a sensitivity of 87.99%, an F1-score of 89.34%, and a precision of 92.94%. Although these results are lower than those of ResNet50, VGG19 still provides reasonable accuracy and precision for maize leaf disease classification.

DenseNet121 outperformed ResNet50 in terms of accuracy, achieving an accuracy of 97.14%, a sensitivity of 96.60%, an F1-score of 96.80%, and a precision of 97.02%. This suggests that DenseNet121 is a highly accurate and reliable maize leaf disease classification model.

InceptionV3 also achieved high accuracy, with an accuracy of 97.62%, a sensitivity of 96.05%, an F1-score of 96.87%, and a precision of 98.01%. These results suggest that InceptionV3 is a reliable maize leaf disease classification model, particularly when high precision is required.

EfficientNet B6 achieved the highest accuracy of 98.10%, a sensitivity of 98.28%, an F1-score of 97.87%, and a precision of 97.60%. This indicates that EfficientNet B6 is a highly accurate and reliable maize leaf disease classification model. Among the models tested on the original dataset, EfficientNet B6 achieved the highest accuracy of 98.10%, followed by EfficientNet B2 with 97.62% accuracy. VGG19 achieved the lowest accuracy of 91.43%.

Table 3 Performance metrics of deep learning models for the original dataset

Transfer Learning Models	Avg Acc (%)	Avg Sen (%)	F1-Score (%)	Avg Pre (%)
ResNet50	96.67	95.70	95.67	95.66
VGG19	91.43	87.99	89.34	92.94
DenseNet121	97.14	96.60	96.80	97.02
InceptionV3	97.62	96.05	96.87	98.01
EfficientNet B0	95.71	95.25	95.33	95.51
EfficientNet B1	96.19	95.17	95.65	96.23
EfficientNet B2	97.62	96.92	97.18	97.46
EfficientNet B3	97.14	97.00	96.81	96.64
EfficientNet B4	95.24	93.84	94.09	94.38
EfficientNet B5	96.67	96.52	96.64	96.89
<b>EfficientNet B6</b>	<b>98.10</b>	<b>98.28</b>	<b>97.87</b>	<b>97.60</b>
EfficientNet B7	97.14	96.03	96.27	96.54

The augmented dataset originated from the original dataset by integrating diverse image augmentation strategies. This augmented dataset served as the training and evaluation set for models identical to those used with the original data. Notably, when tested on the augmented dataset, the ResNet50 model exhibited an impressive accuracy rate of 98.32%. Additionally, the model showcased a commendable sensitivity of 98.55%, underscoring its proficiency in accurately detecting diseased leaf images. Nonetheless, the precision of this model stood at 97.22%, suggesting instances where it misclassified healthy leaves as diseased, leading to certain false positives.

VGG19, achieved an accuracy of 97.64% on the augmented dataset. Its sensitivity was 96.64%, lower than ResNet50, but its precision was higher at 97.27%. This suggests that VGG19 was better at correctly identifying diseased leaves but had a higher chance of incorrectly classifying healthy leaves as diseased.

DenseNet121 achieved an accuracy of 96.97% on the augmented dataset, with a sensitivity of 96.36% and a precision of 95.84%. Its F1-score was 96.08%, which measures the balance between accuracy and sensitivity. DenseNet121 had a lower sensitivity than ResNet50 and VGG19, but it had a higher precision.

InceptionV3 achieved an accuracy of 97.31% on the augmented dataset, with a sensitivity of 97.36% and a precision of 96.26%. Its F1-score was 96.75%, similar to VGG19 but lower than ResNet50. InceptionV3 had a higher sensitivity compared to DenseNet121 but a lower precision.

EfficientNet models, including B0, B1, B2, B3, B4, B5, B6, and B7, achieved high accuracies ranging from 97.98% to 99.66% on the augmented dataset. The models had high sensitivities ranging from 97.26% to 99.71%, which indicates that they could correctly identify a high percentage of the images affected by the diseases. Among the models tested on the augmented dataset, EfficientNet B3 achieved the highest accuracy of 99.66%, followed by EfficientNet B6 with 98.99%



accuracy. VGG19 achieved the lowest accuracy of 97.64%.

Table 4 Performance metrics of deep learning models for the augmented dataset

Transfer Learning Models	Avg Acc (%)	Avg Sen (%)	F1-Score (%)	Avg Pre (%)
ResNet50	98.32	98.55	97.79	97.22
VGG19	97.64	96.64	96.93	97.27
DenseNet121	96.97	96.36	96.08	95.84
InceptionV3	97.31	97.36	96.75	96.26
EfficientNet B0	97.98	97.26	97.41	97.57
EfficientNet B1	98.32	98.19	97.89	97.62
EfficientNet B2	97.98	97.26	97.41	97.57
<b>EfficientNet B3</b>	<b>99.66</b>	<b>99.71</b>	<b>99.55</b>	<b>99.39</b>
EfficientNet B4	97.98	97.92	97.47	97.07
EfficientNet B5	98.32	98.22	97.90	97.62
EfficientNet B6	98.99	98.79	98.63	98.48
EfficientNet B7	98.32	97.54	97.69	97.85

The accuracy values of all models in the original dataset are presented in Figure 10, while Figure 11 displays the accuracy values in the augmented dataset. Accuracy is measured by dividing the number of correctly classified samples by the total number of samples. The EfficientNet B6 model recorded the highest accuracy of 98.10% in the original dataset, while the EfficientNet B3 model achieved the highest accuracy of 99.66% in the augmented dataset. Conversely, VGG19 and DenseNet121 had the lowest accuracy values in both datasets. These findings indicate that the accuracy value in the augmented dataset is greater than that of the original dataset.

In summary, the deep learning frameworks examined in this research exhibit encouraging outcomes in identifying maize leaf diseases through image analysis. Notably, the EfficientNet architectures consistently manifest elevated accuracy levels across the initial and augmented datasets. Furthermore, the augmented dataset notably enhances the efficacy of most models, underscoring the pivotal role of image augmentation methodologies in refining the accuracy of deep learning frameworks. Figure 10 showcases the accuracy metrics for all models based on the original dataset, whereas Figure 11 illustrates the accuracy figures from the augmented dataset. Accuracy is computed by the ratio of accurately classified samples to the total sample count. Noteworthy, the EfficientNet B6 model led with a peak accuracy of 98.10% when evaluated against the original

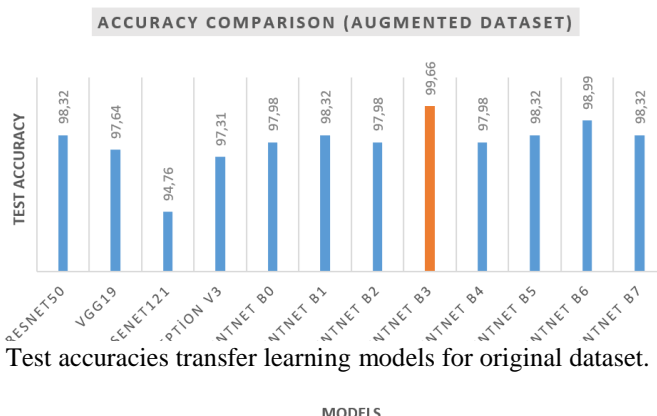


Figure 10 Test accuracies transfer learning models for original dataset.

dataset, whereas the EfficientNet B3 model excelled with an accuracy of 99.66% on the augmented dataset. In contrast, VGG19 and DenseNet121 consistently exhibited the least accuracy across both datasets. Such results strongly suggest that the augmented dataset consistently yields higher accuracy rates than its original counterpart.

Figure 1 Test accuracies transfer learning models for the augmented dataset.

Table 5 presents the performance metrics, including TP, FP, TN, FN, sensitivity, accuracy, F1-Score, and precision values, for each class of the EfficientNet B6 model, which demonstrated superior performance in the original data set. On the other hand, Table 6 displays the corresponding performance metrics for each class of the EfficientNet B3 model, which exhibited the best performance in the augmented data set, including TP, FP, TN, FN, sensitivity, F1-Score, and precision values.

The first model, EfficientNet B6, was trained on the original dataset, while the second model, EfficientNet B3, was trained on an augmented dataset. Let's first look at the results of EfficientNet B6 on the original dataset. For Blight, the model achieved a TP of 54, TN of 152, FP of 0, and FN of 4, resulting in a sensitivity of 93.10, F1-score of 96.43, and precision of 100. For Common Rust, the model achieved a TP of 66, TN of 140, FP of 2, and FN of 0, resulting in a sensitivity of 100, F1-score of 98.51, and a precision of 97.06. For the Gray leaf spot, the model achieved a TP of 28, TN of 178, FP of 2, and FN of 0, resulting in a sensitivity of 100, F1-score of 96.55, and precision of 93.33. Lastly, for Healthy, the model achieved a TP of 58, TN of 148, FP of 0, and FN of 0, resulting in a sensitivity of 100, F1-score of 100, and precision of 100.

Table 5 EfficientNet B6 Model original dataset classification performance

Class	TP	TN	FP	FN	Sen(%)	F1-Score(%)	Pre(%)
Blight	54	152	0	4	93.10	96.43	100.00
Common Rust	66	140	2	0	100.00	98.51	97.06
Gray Leaf Spot	28	178	2	0	100.00	96.55	93.33
Healthy	58	148	0	0	100.00	100.00	100.00

Now, let's look at the results of EfficientNet B3 on the augmented dataset. For Blight, the model achieved a TP of 84, TN of 212, FP of 0, and FN of 1, resulting in a sensitivity of 98.82, F1-score of 99.81, and precision of 100. For Common Rust, the model achieved a TP of 91, TN of 205, FP of 0, and FN of 0, resulting in a sensitivity of 100, F1-score of 100, and precision of 100. For Gray leaf spot, the model achieved a TP of 40, TN of 256, FP of 1, and FN of 0, resulting in a sensitivity of 100, F1-score of 98.77, and precision of 97.56. Lastly, for Healthy, the model achieved a TP of 81, TN of 215, FP of 0, and FN of 0, resulting in a sensitivity of 100, F1-score of 100, and precision of 100.

Table 6 EfficientNet B3 Model Augmented Dataset Classification Performance

Class	TP	TN	FP	FN	Sen(%)	F1-Score(%)	Pre(%)
Blight	84	212	0	1	98.82	99.81	100.00
Common Rust	91	205	0	0	100.00	100.00	100.00
Gray Leaf Spot	40	256	1	0	100.00	98.77	97.56
Healthy	81	215	0	0	100.00	100.00	100.00

Comparing the two models, we can see that the model trained on the augmented dataset, EfficientNet B3, outperformed the model trained on the original dataset, EfficientNet B6. In particular, EfficientNet B3 achieved higher sensitivities for all four classes, indicating a better ability to classify diseased leaves correctly. Additionally, EfficientNet B3 achieved higher F1 scores for three out of four classes, indicating a better balance between precision and recall. Lastly, EfficientNet B3 achieved perfect precision for all four classes, indicating that the model made no false positive predictions. In conclusion, EfficientNet B3 trained on an augmented dataset showed superior performance in classifying maize leaf diseases compared to EfficientNet B6 trained on the original dataset. The results demonstrate the importance of data augmentation in increasing the quality of the dataset and improving the performance of the model. The confusion matrices for the models EfficientNet B6 for the original dataset and EfficientNet B3 for the augmented dataset are given in Figure 12 and Figure 13, respectively. Confusion matrices of both models were compared to evaluate the classification performance. The original dataset model, EfficientNet B6, had a sensitivity of 93.10%, 100%, 100%, and 100% for Blight, Common Rust, Gray leaf spot, and Healthy, respectively. The model correctly classified Blight, Common Rust, and Healthy leaf diseases with high accuracy. However, it struggled with the Gray leaf spot, with only 28 out of 30 images correctly classified, resulting in a sensitivity of 93.10%.

On the other hand, the augmented dataset model, EfficientNet B3, achieved a sensitivity of 98.82%, 100%, 100%, and 100% for Blight, Common Rust, Gray leaf spot, and Healthy, respectively. This model showed better performance than the original dataset model in all four classes of diseases, with higher sensitivity and F1-score. The model correctly classified all images of Common Rust and Healthy, and all but one image of Blight. The Gray leaf spot classification improved significantly, with 40 out of 40 images correctly classified, resulting in a sensitivity of 100%.

Overall, the augmented dataset model, EfficientNet B3, showed better performance in classifying maize leaf diseases than the original dataset model, EfficientNet B6. The improved sensitivity and F1-score of the augmented dataset model are particularly notable for Gray leaf spot classification. The results suggest that the use of augmented datasets can improve the performance of deep learning models in image-based classification of maize leaf diseases.

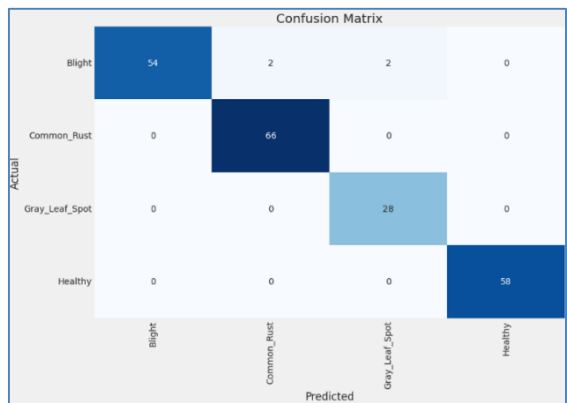


Figure 2 EfficientNet B6 Confusion Matrix for original dataset

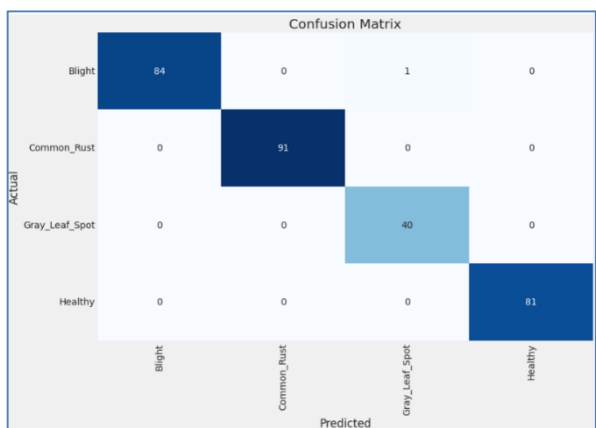


Figure 3 EfficientNet B3 Confusion Matrix for augmented dataset

The results for the original dataset and enriched dataset models of EfficientNet B6 and B3 are presented in Figures 14 and 15, respectively. The effectiveness of the early stopping approach in maintaining higher performance values is demonstrated by the point at which the validation loss begins to decrease. The EfficientNet B6 model achieved its best validation loss and accuracy values in the 42nd and 29th epochs, respectively, as illustrated in Figure 14. Similarly, the EfficientNet B3 model attained its optimal validation loss and accuracy values in the 50th and 26th epochs, respectively, as shown in Figure 15.

As shown in Figure 14 a and Figure 15 a, as the number of epochs increases, the decrease in both training and validation loss is generally due to the increasing learning capacity of the model. With more epochs, the model is exposed to more data, allowing it to gain more insights, resulting in better generalization and lower loss values overall. Additionally, long-term training enables the model to learn both general patterns and finer details over time. Also, increasing epochs increases the model's resistance to overfitting, thus helping to reduce validation loss. It is very important to stop training at the point where the model is performing at its best. The EfficientNet B6 model trained with the original data set reached its best value in the 42nd epoch, while the EfficientNet B3 model using the augmented data set reached its best value in the 50th epoch.



Figure 4 a-b ) EfficientNet B6 training and validation loss and accuracy in original dataset

As the number of epochs in Figures 14 b and 15 b increases, training and validation accuracy values increase due to the improved learning capacity of the model. With more epochs, the model is exposed to more data, which allows it to learn general patterns and data properties better, resulting in higher accuracy values. In addition, increasing epochs often contribute to better generalization of the model, initially better adjusting the training data and subsequently improving the generalization ability, leading to higher training and validation accuracy values. Monitoring accuracy values during training and stopping at the optimum performance point ensures the best results. The EfficientB6 model trained with the original data set reached its best value in the 29th epoch, while the EfficientNetB3 model using the augmented data set reached its best value in the 26th epoch.

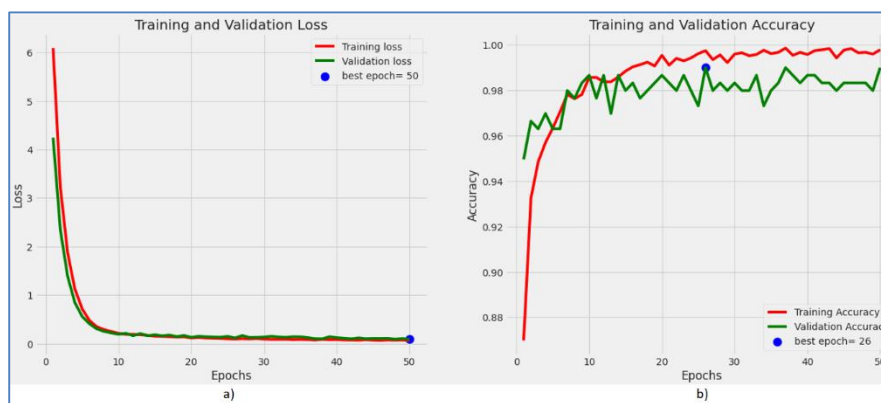


Figure 5 a-b ) EfficientNet B3 training and validation loss and accuracy in the augmented dataset

The findings indicate that both the EfficientNet B3 and EfficientNet B6 models achieved high accuracy values of 98% and 99%, respectively, on both the original and augmented datasets. Furthermore, the sensitivity values of these models were also high at 98% and 99%, respectively. These two models demonstrated the highest level of performance among all the models evaluated. The augmented dataset led to an increase in accuracy and sensitivity values across all models. The EfficientNet B3 model, which performed the best on the augmented dataset, exhibited a 2% increase in accuracy and a 3% increase in precision, highlighting the positive impact of increased data on model predictions.

The total number of classification errors for all models is shown in Table 7. In this study, various models, including ResNet50, VGG19, DenseNet121, InceptionV3, and EfficientNet B0 to B7, were evaluated using an original dataset of 210 images and an augmented dataset of 297 images. The aim was to compare the models' classification accuracy and false prediction rate on both datasets.

Results from the original dataset showed that EfficientNet B6 exhibited the best performance with only four false predictions out of 210 images. EfficientNet B3, InceptionV3, and DenseNet121 followed closely with 5 to 6 false predictions. ResNet50, EfficientNet B5, and EfficientNet B7 had a moderate false prediction rate, with 7 to 9 false predictions. VGG19 and EfficientNet B1 had the highest false prediction rate, with 18 and 8 false predictions, respectively.

However, the augmented dataset produced slightly different results. EfficientNet B3 demonstrated the best performance, with only one false prediction out of 297 images. EfficientNet B6 and VGG19 also performed well, with only 3 and 7 false predictions. DenseNet121 and InceptionV3 had a moderate false prediction rate with 8 to 9 false predictions, while ResNet50 and EfficientNet B0 to B2, B4, and B7 had a higher false prediction rate ranging from 5 to 6.

Overall, results from both datasets demonstrate that EfficientNet B3 and B6 models are suitable for classifying maize leaf diseases. EfficientNet B3 is particularly promising as it achieved the lowest false prediction rate on the augmented dataset.

In general, the augmented dataset improved the models' accuracy and reduced their false prediction rate compared to the original dataset.

In the discussion, we can highlight several key points:

Performance discrepancies between models: The data reveals variations in false prediction rates across different models. For instance, while ResNet50 and DenseNet121 exhibit relatively low false prediction rates in the original dataset compared to VGG19 and InceptionV3, the situation changes in the augmented dataset where VGG19 and InceptionV3 show a decrease in false predictions. Impact of data augmentation: Comparing false prediction rates between the original and augmented datasets sheds light on the effectiveness of data augmentation techniques. In some cases, such as with DenseNet121 and B5-B7 models, false prediction rates increase in the augmented dataset, suggesting that certain augmentation strategies may not universally improve model performance. Model robustness and generalization: The discrepancy in false prediction rates among different models highlights variations in model robustness and generalization capabilities. Models that exhibit consistent performance across both datasets, such as B2 and B3, may indicate more robust architectures that generalize well to augmented data. Potential for further investigation: The observed differences in false prediction rates present avenues for further investigation. Researchers could delve deeper into understanding why certain models perform better in augmented datasets while others do not, leading to insights that could enhance model training strategies and data augmentation techniques. Implications for real-world applications: Discussing the impact of these findings for real-world applications is essential. Understanding model performance under different conditions, such as augmented datasets, is crucial for deploying reliable and robust systems in practical scenarios, such as wildlife monitoring or medical imaging. By incorporating these points into the discussion, the paper can provide a comprehensive analysis of the observed results and their implications for the field of machine learning and computer vision.

In conclusion, the study highlights the importance of choosing an appropriate deep-learning model for classifying maize leaf diseases. The findings suggest that using an augmented dataset can help to improve the accuracy of the models.

Table 7 False prediction values for Transfer Learning Models

	ResNet50	VGG19	DenseNet121	Inception V3	B0	B1	B2	B3	B4	B5	B6	B7
Total False Prediction in the original dataset	7	18	6	5	9	8	5	6	10	7	4	6
Total False Prediction in Augmented Dataset	5	7	9	8	6	5	6	1	6	5	3	5

### 5. Conclusion

Within the agricultural sector, identifying and categorizing plant diseases holds paramount significance. Timely identification averts extensive crop devastation and safeguards farmers from substantial economic setbacks. Consequently, the adoption of machine learning techniques to autonomously discern plant diseases has surged in prominence recently.

In the present study, we conducted a performance comparison of EfficientNet, ResNet50, VGG19, DenseNet121, and Inception V3 models for the classification of maize leaf diseases, including Blight, Common Rust, Gray leaf spot, and Healthy images. The assessment was carried out using both the original and augmented datasets.

The results of the original dataset trained EfficientNet B6 model showed good performance in detecting all four categories of maize leaf diseases, with a sensitivity of 100% for Common Rust and Healthy images. However, the model showed a relatively lower sensitivity of 93.10% for Blight and 96.55% for Gray leaf spot images. The F1 scores were relatively high for all four categories, with a maximum of 100% for Healthy images. The precision of the model was perfect for Blight and Healthy photos, while it was slightly lower for Common Rust and Gray leaf spot images.

On the other hand, the EfficientNet B3 model trained on the augmented dataset showed better results, with a higher sensitivity for all four categories of maize leaf diseases. The model's sensitivity was 98.82% for Blight, 100% for Common Rust and Healthy images, and 97.56% for Gray leaf spot images. The F1 scores were high for all categories, with a maximum of 100% for Healthy images. The precision of the model was perfect for all four categories of maize leaf diseases.

Overall, our results demonstrate that using augmented datasets can significantly improve the performance of deep-learning models for the classification of maize leaf diseases. The EfficientNet B3 model trained on the augmented dataset showed better sensitivity and precision results than the EfficientNet B6 model trained on the original dataset. These findings highlight the importance of using augmented datasets in deep learning algorithms for accurate and efficient classification of plant diseases, which can ultimately help in the early detection and prevention of widespread crop damage.

## References

- [1] S. Sankaran, A. Mishra, R. Ehsani and C. Davis, “A review of advanced techniques for detecting plant diseases,” *Comput Electron Agric*, vol. 72, no. 1, pp. 1–13, Jun. 2010, doi: 10.1016/j.compag.2010.02.007.
- [2] S. Mishra, R. Sachan and D. Rajpal, “Deep convolutional neural network based detection system for real-time corn plant disease recognition,” in *Procedia Computer Science*, Elsevier B.V., 2020, pp. 2003–2010. doi: 10.1016/j.procs.2020.03.236.
- [3] D. Ozdemir and M. S. Kunduraci, “Comparison of deep learning techniques for classification of the insects in order level with mobile software application,” *IEEE Access*, vol. 10, pp. 35675–35684, 2022, doi: 10.1109/ACCESS.2022.3163380.
- [4] M. Akın, A. Dağdelen, R. N. Eğinme and D. Özdemir, “doğada kendiliğinden yetişen mantar türlerinin derin öğrenme ile tespiti,” *Eskişehir Türk Dünyası Uygulama ve Araştırma Merkezi Bilişim Dergisi*, Dec. 2023, doi: 10.53608/estudambilisim.1319221.
- [5] D. Özdemir and N. N. Arslan, “Analysis of Deep transfer learning methods for early diagnosis of the Covid-19 disease with Chest X-ray images,” *Düzce Üniversitesi Bilim ve Teknoloji Dergisi*, vol. 10, no. 2, pp. 628–640, Apr. 2022, doi: 10.29130/dubited.976118.
- [6] E. Şahin, D. Özdemir and H. Temurtaş, “Multi-objective optimization of ViT architecture for efficient brain tumor classification,” *Biomed Signal Process Control*, vol. 91, May 2024, doi: 10.1016/j.bspc.2023.105938.
- [7] N. N. Arslan, D. Ozdemir and H. Temurtas, “ECG heartbeats classification with dilated convolutional autoencoder,” *Signal Image Video Process*, Feb. 2023, doi: 10.1007/s11760-023-02737-2.
- [8] B. Guler Ayyildiz, R. Karakis, B. Terzioglu and D. Ozdemir, “Comparison of deep learning methods for the radiographic detection of patients with different periodontitis stages,” *Dentomaxillofac Radiol*, vol. 53, no. 1, pp. 32–42, Jan. 2024, doi: 10.1093/dmfr/twad003.
- [9] D. Ozdemir and M. Emin UGUR, “Deniz Yildizlari Vocational and Technical Anatolian High School Ministry of National Education Kocaeli.”
- [10] K. P. Ferentinos, “Deep learning models for plant disease detection and diagnosis,” *Comput Electron Agric*, vol. 145, pp. 311–318, Feb. 2018, doi: 10.1016/j.compag.2018.01.009.
- [11] F. Jiang *et al.*, “Artificial intelligence in healthcare: Past, present and future,” *Stroke and Vascular Neurology*, vol. 2, no. 4. BMJ Publishing Group, pp. 230–243, Dec. 01, 2017. doi: 10.1136/svn-2017-000101.
- [12] P. Dong, K. Li, M. Wang, F. Li, W. Guo and H. Si, “Maize Leaf Compound Disease Recognition Based on Attention Mechanism,” *Agriculture (Switzerland)*, vol. 14, no. 1, Jan. 2024, doi: 10.3390/agriculture14010074.
- [13] R. Ahila Priyadharshini, S. Arivazhagan, M. Arun and A. Mirnalini, “Maize leaf disease classification using deep convolutional neural networks,” *Neural Comput Appl*, vol. 31, no. 12, 2019, doi: 10.1007/s00521-019-04228-3.
- [14] V. Sharma, A. K. Tripathi, P. Daga, M. Nidhi and H. Mittal, “ClGanNet: A novel method for maize leaf disease identification using ClGan and deep CNN,” *Signal Process Image Commun*, vol. 120, Jan. 2024, doi: 10.1016/j.image.2023.117074.
- [15] H. Al-Hiary, S. Bani-Ahmad, M. Reyalat, M. Braik and Z. Alrahamneh, “Fast and Accurate Detection and Classification of Plant Diseases,” 2011.
- [16] P. Revathi and M. Hemalatha, “Advance computing enrichment evaluation of cotton leaf spot disease detection using Image Edge detection,” in *2012 3rd International Conference on Computing, Communication and Networking Technologies, ICCCNT 2012*, 2012. doi: 10.1109/ICCCNT.2012.6395903.
- [17] U. Mokhtar, M. A. S. Ali, A. E. Hassanien and H. Hefny, “Identifying two of tomatoes leaf viruses using support vector machine,” in *Advances in Intelligent Systems and Computing*, Springer Verlag, 2015, pp. 771–782. doi: 10.1007/978-81-322-2250-7\_77.
- [18] X. E. Pantazi, D. Moshou, A. A. Tamouridou and S. Kasderidis, “Leaf disease recognition in vine plants based on local binary patterns and one class support vector machines,” in *IFIP Advances in Information and Communication Technology*, Springer New York LLC, 2016, pp. 319–327. doi: 10.1007/978-3-319-44944-9\_27.
- [19] A. Johannes *et al.*, “Automatic plant disease diagnosis using mobile capture devices, applied on a wheat use case,” *Comput Electron Agric*, vol. 138, pp. 200–209, Jun. 2017, doi: 10.1016/j.compag.2017.04.013.
- [20] J. Chen, H. Yin and D. Zhang, “A self-adaptive classification method for plant disease detection using

- GMDH-Logistic model,” *Sustainable Computing: Informatics and Systems*, vol. 28, Dec. 2020, doi: 10.1016/j.suscom.2020.100415.
- [21] Y. Lecun, Y. Bengio and G. Hinton, “Deep learning,” *Nature*, vol. 521, no. 7553. Nature Publishing Group, pp. 436–444, May 27, 2015. doi: 10.1038/nature14539.
- [22] H. C. Altunay and Z. Albayrak, “A hybrid CNN + LSTMbased intrusion detection system for industrial IoT networks,” *Engineering Science and Technology, an International Journal*, vol. 38, Feb. 2023, doi: 10.1016/j.jestch.2022.101322.
- [23] M. Çakmak and Z. Albayrak, “AFCC-r: Adaptive Feedback Congestion Control Algorithm to Avoid Queue Overflow in LTE Networks,” *Mobile Networks and Applications*, vol. 27, no. 5, 2022, doi: 10.1007/s11036-022-02011-8.
- [24] R. İncir and F. Bozkurt, “A study on effective data preprocessing and augmentation method in diabetic retinopathy classification using pre-trained deep learning approaches,” *Multimed Tools Appl*, vol. 83, no. 4, pp. 12185–12208, Jan. 2023, doi: 10.1007/S11042-023-15754-7/TABLES/7.
- [25] D. Shen, G. Wu and H.-I. Suk, “Deep Learning in Medical Image Analysis,” 2017, doi: 10.1146/annurev-bioeng-071516.
- [26] S. Nahzat, F. Bozkurt and M. Yağanoğlu, “White Blood Cell Classification Using Convolutional Neural Network,” *Journal of Scientific Technology and Engineering Research*, 2022, doi: 10.53525/jster.1018213.
- [27] F. Bozkurt, “A deep and handcrafted features-based framework for diagnosis of COVID-19 from chest x-ray images,” *Concurr Comput*, vol. 34, no. 5, 2022, doi: 10.1002/cpe.6725.
- [28] A. Ahmad, D. Saraswat and A. El Gamal, “A survey on using deep learning techniques for plant disease diagnosis and recommendations for development of appropriate tools,” *Smart Agricultural Technology*, vol. 3. 2023. doi: 10.1016/j.atech.2022.100083.
- [29] J. Chen, A. Zeb, Y. A. Nanekaran and D. Zhang, “Stacking ensemble model of deep learning for plant disease recognition,” *J Ambient Intell Humaniz Comput*, vol. 14, no. 9, 2023, doi: 10.1007/s12652-022-04334-6.
- [30] J. Chen, J. Chen, D. Zhang, Y. Sun and Y. A. Nanekaran, “Using deep transfer learning for image-based plant disease identification,” *Comput Electron Agric*, vol. 173, Jun. 2020, doi: 10.1016/j.compag.2020.105393.
- [31] M. Nawaz, T. Nazir, A. Javed, S. Tawfik Amin, F. Jeribi and A. Tahir, “CoffeeNet: A deep learning approach for coffee plant leaves diseases recognition,” *Expert Syst Appl*, vol. 237, 2024, doi: 10.1016/j.eswa.2023.121481.
- [32] E. C. Too, L. Yujian, S. Njuki and L. Yingchun, “A comparative study of fine-tuning deep learning models for plant disease identification,” *Comput Electron Agric*, vol. 161, pp. 272–279, Jun. 2019, doi: 10.1016/j.compag.2018.03.032.
- [33] G. Geetharamani and A. P. J., “Identification of plant leaf diseases using a nine-layer deep convolutional neural network,” *Computers and Electrical Engineering*, vol. 76, pp. 323–338, Jun. 2019, doi: 10.1016/j.compeleceng.2019.04.011.
- [34] B. Chang, Y. Wang, X. Zhao, G. Li and P. Yuan, “A general-purpose edge-feature guidance module to enhance vision transformers for plant disease identification[Formula presented],” *Expert Syst Appl*, vol. 237, 2024, doi: 10.1016/j.eswa.2023.121638.
- [35] A. L. Latifah, Lembaga Ilmu Pengetahuan Indonesia. Research Center for Informatics, Institute of Electrical and Electronics Engineers. Indonesia Section and Institute of Electrical and Electronics Engineers, *2018 International Conference on Computer, Control, Informatics and its Applications: “Recent Challenges in Machine Learning for Computing Applications” : proceedings : November 1st-2nd, 2018, Tangerang, Indonesia*.
- [36] S. M. Hassan, M. Jasinski, Z. Leonowicz, E. Jasinska and A. K. Maji, “Plant disease identification using shallow convolutional neural network,” *Agronomy*, vol. 11, no. 12, Dec. 2021, doi: 10.3390/agronomy11122388.
- [37] Ü. Atila, M. Uçar, K. Akyol and E. Uçar, “Plant leaf disease classification using EfficientNet deep learning model,” *Ecol Inform*, vol. 61, Mar. 2021, doi: 10.1016/j.ecoinf.2020.101182.
- [38] A. M. Fayyaz *et al.*, “Leaf blights detection and classification in large scale applications,” *Intelligent Automation and Soft Computing*, vol. 31, no. 1, pp. 507–522, 2022, doi: 10.32604/IASC.2022.016392.
- [39] A. Elaraby, W. Hamdy and M. Alruwaili, “Optimization of deep learning model for plant disease detection using particle swarm optimizer,” *Computers, Materials and Continua*, vol. 71, no. 2, pp. 4019–4031, 2022, doi: 10.32604/cmc.2022.022161.

- [40] A. N. Özalp and Z. Albayrak, “Detecting cyber attacks with high-frequency features using machine learning algorithms,” 2023.
- [41] C. Tan, F. Sun, T. Kong, W. Zhang, C. Yang and C. Liu, “A survey on deep transfer learning,” in *Lecture Notes in Computer Science (including subseries Lecture Notes in Artificial Intelligence and Lecture Notes in Bioinformatics)*, Springer Verlag, 2018, pp. 270–279. doi: 10.1007/978-3-030-01424-7\_27.
- [42] K. He, X. Zhang, S. Ren and J. Sun, “Deep Residual Learning for Image Recognition.” [Online]. Available: <http://image-net.org/challenges/LSVRC/2015/>
- [43] O. Russakovsky *et al.*, “ImageNet Large Scale Visual Recognition Challenge,” *Int J Comput Vis*, vol. 115, no. 3, pp. 211–252, Dec. 2015, doi: 10.1007/s11263-015-0816-y.
- [44] K. Simonyan and A. Zisserman, “Very deep convolutional networks for large-scale image recognition,” 2015. [Online]. Available: <http://www.robots.ox.ac.uk/>
- [45] G. Huang, Z. Liu, L. van der Maaten and K. Q. Weinberger, “Densely Connected Convolutional Networks.” [Online]. Available: <https://github.com/liuzhuang13/DenseNet>.
- [46] A. Sardar, A. Issa and Z. Albayrak, “DDoS Attack Intrusion Detection System Based on Hybridization of CNN and LSTM,” 2023.
- [47] Q. Ji, J. Huang, W. He and Y. Sun, “Optimized deep convolutional neural networks for identification of macular diseases from optical coherence tomography images,” *Algorithms*, vol. 12, no. 3, 2019, doi: 10.3390/a12030051.
- [48] C. Szegedy, V. Vanhoucke, S. Ioffe, J. Shlens and Z. Wojna, “Rethinking the Inception Architecture for Computer Vision,” Dec. 2015, [Online]. Available: <http://arxiv.org/abs/1512.00567>
- [49] C. Szegedy, V. Vanhoucke, S. Ioffe, J. Shlens and Z. Wojna, “Rethinking the Inception Architecture for Computer Vision,” Dec. 2015, [Online]. Available: <http://arxiv.org/abs/1512.00567>
- [50] M. Sandler, A. Howard, M. Zhu, A. Zhmoginov and L.-C. Chen, “MobileNetV2: Inverted Residuals and Linear Bottlenecks,” Jan. 2018, [Online]. Available: <http://arxiv.org/abs/1801.04381>
- [51] M. Tan and Q. V. Le, “EfficientNet: Rethinking Model Scaling for Convolutional Neural Networks,” May 2019, [Online]. Available: <http://arxiv.org/abs/1905.11946>

#### **Conflict of Interest Notice**

The authors declare that there is no conflict of interest regarding the publication of this paper.

#### **Ethical Approval and Informed Consent**

It is declared that during the preparation process of this study, scientific and ethical principles were followed, and all the studies benefited from are stated in the bibliography.

#### **Availability of data and material**

Not applicable.

#### **Plagiarism Statement**

This article has been scanned by iThenticate™.